Title
Sensitivity of summer ensembles of fledgling superparameterized U.S. mesoscale convective systems to cloud resolving model microphysics and grid configuration

Journal
Journal of Advances in Modeling Earth Systems, 8(2)

ISSN
1942-2466

Authors
Elliott, Elizabeth J
Yu, Sungduk
Kooperman, Gabriel J
et al.

Publication Date
2016-06-01

DOI
10.1002/2015ms000567

Peer reviewed

AGU PUBLICATIONS

Journal of Advances in Modeling Earth Systems

RESEARCH ARTICLE
10.1002/2015MS000567

Key Points:
- Internal variability of U.S. MCS events dominate CRM sensitivities in superparameterized CAM
- Need ensembles of 100+ storms to detect sensitivities and tune superparameterized physics

Correspondence to:
M. S. Pritchard,
mspritch@uci.edu

Citation:
Elliott, E. J, S. Yu, G. J. Kooperman, H. Morrison, M. Wang, and M. S. Pritchard (2016), Sensitivity of summer ensembles of fledgling superparameterized U.S. mesoscale convective systems to cloud resolving model microphysics and grid configuration, *J. Adv. Model. Earth Syst.*, *8*, 634–649, doi:10.1002/2015MS000567.

Received 18 OCT 2015
Accepted 7 APR 2016
Accepted article online 12 APR 2016
Published online 1 MAY 2016

Sensitivity of summer ensembles of fledgling superparameterized U.S. mesoscale convective systems to cloud resolving model microphysics and grid configuration

Elizabeth J. Elliott[1], Sungduk Yu[1], Gabriel J. Kooperman[1], Hugh Morrison[2], Minghuai Wang[3,4], and Michael S. Pritchard[1]

[1]Department of Earth System Science, University of California Irvine, Irvine, California, USA, [2]National Center for Atmospheric Research, Boulder, Colorado, USA, [3]Institute for Climate and Global Change Research, School of Atmospheric Sciences, Nanjing University, Nanjing, China, [4]Jiangsu Collaborative Innovation Center of Climate Change, Nanjing, China

Abstract The sensitivities of simulated mesoscale convective systems (MCSs) in the central U.S. to microphysics and grid configuration are evaluated here in a global climate model (GCM) that also permits global-scale feedbacks and variability. Since conventional GCMs do not simulate MCSs, studying their sensitivities in a global framework useful for climate change simulations has not previously been possible. To date, MCS sensitivity experiments have relied on controlled cloud resolving model (CRM) studies with limited domains, which avoid internal variability and neglect feedbacks between local convection and larger-scale dynamics. However, recent work with superparameterized (SP) GCMs has shown that eastward propagating MCS-like events are captured when embedded CRMs replace convective parameterizations. This study uses a SP version of the Community Atmosphere Model version 5 (SP-CAM5) to evaluate MCS sensitivities, applying an objective empirical orthogonal function algorithm to identify MCS-like events, and harmonizing composite storms to account for seasonal and spatial heterogeneity. A five-summer control simulation is used to assess the magnitude of internal and interannual variability relative to 10 sensitivity experiments with varied CRM parameters, including ice fall speed, one-moment and two-moment microphysics, and grid spacing. MCS sensitivities were found to be subtle with respect to internal variability, and indicate that ensembles of over 100 storms may be necessary to detect robust differences in SP-GCMs. These results emphasize that the properties of MCSs can vary widely across individual events, and improving their representation in global simulations with significant internal variability may require comparison to long (multidecadal) time series of observed events rather than single season field campaigns.

1. Introduction

Mesoscale convective systems (MCSs) in the central U.S. can deliver up to half of warm season accumulated rainfall in the region, and are associated with extreme flooding events. However, MCSs are governed by exotic physics of organized convection that are not captured by conventional deep convection parameterizations [*Moncrieff and Liu*, 2006], and thus are missing in most global climate models (GCMs) even with a high-resolution horizontal grid size of O(25 km) [*Bacmeister et al.*, 2014]. As a result, the climate change response of these storms and the rainfall they generate remains uncertain.

Superparameterized (SP) GCMs, which replace traditional convective parameterizations with embedded cloud resolving models (CRMs) in each grid column of a host GCM [*Grabowski*, 2001], such as the SP version of the Community Atmosphere Model (CAM) [*Khairoutdinov and Randall*, 2001], have been shown to simulate an organized MCS-like storm signal. Unlike conventional versions of CAM, which tend to produce frequent local convection in the early afternoon, SP-CAM captures intermittent nocturnal convective systems that propagate eastward across the central U.S. [*Pritchard et al.*, 2011].

Given the dynamic limitations of the two-dimensional CRM configuration used in SP-CAM, which can distort MCS physics relative to three-dimensional configurations in stand-alone CRM simulations [*Schlesinger*, 1984; *Weisman et al.*, 1988; *Nicholls and Weissbluth*, 1988; *Wandishin et al.*, 2008; *Wandishin et al.*, 2010], it is somewhat surprising that SP-CAM is able to produce these propagating systems. While it may be tempting to imagine the individual CRM arrays in SP-CAM as self-contained models responding to an external large-scale forcing, as is the case for limited-domains CRM studies, the interactions across the CRM-GCM interface are in fact more complicated than that. *Pritchard et al*. [2011] showed that SP-CAM simulates MCS-like structures that span scales larger than an individual CRM array, allowing CRMs to interact with and feedback on GCM-scale three-dimensional dynamics. The physics permitted by the coupled CRM-GCM framework may not be restricted by the same limitations as purely two-dimensional CRM simulations. Here we treat the embedded CRMs as "parameterizations of convection for the GCM," rather than individual realizations of simulated storms, and evaluate MCS sensitivities as they manifest on GCM scales and interact with the larger climate system.

MCS sensitivities to model implementation have been hypothesized in previous SP-CAM results. The MCS signal differs in intensity and horizontal extent from one version of SP-CAM to the next, revealing the need for further model evaluation and tuning against observations [*Kooperman et al*., 2013, hereinafter K13]. K13 speculated that recent updates in the embedded CRM microphysics parameterizations may have been the primary driver of an important improvement in the MCS-like longwave radiative signal strength in seasonal-scale integrations of the most recent version of SP-CAM (v5.0; hereinafter SP-CAM5). They hypothesized the update from simple bulk microphysics to the new two-moment microphysics scheme contributed to a more realistic composite storm signal in a set of single-season simulations. It is natural to wonder if uncertain microphysics parameters may yet be further tuned to optimize the emerging MCS signal in SP-CAM, which K13 show still has major radiative biases that currently limit the model's usefulness for enhanced regional climate prediction.

Testing the sensitivity of deep convection to one-moment versus two-moment microphysics is especially compelling. By allowing an additional degree of freedom in the particle size distribution, two-moment microphysics brings the potential for a more flexible representation of microphysical processes [*Meyers et al*., 1997; *Seifert and Beheng*, 2001; *Morrison et al*., 2005]. This comes at an increased computational cost which many studies agree is worthwhile for the increased realism of simulated cloud system dynamics [*Milbrandt and Yau*, 2005; *Morrison et al*., 2009; *Dawson et al*., 2010; *Van Weverberg et al*., 2012; *Igel et al*., 2014]. *Bryan and Morrison* [2012, hereinafter BM12] performed a series of simulations of a single squall line over the central U.S. illustrating improved fidelity to data (particularly cloud reflectivity structure, cold pool temperature, and relative humidity) as a result of switching from one-moment to two-moment microphysics.

In addition to the number of microphysical moments, the number and type of dense ice species can produce sensitivities in deep convection [*Fovell and Ogura*, 1988; *McCumber et al*., 1991; *Gilmore et al*., 2004]. In a series of tropical deep convection simulations, *McCumber et al*. [1991] found a three-class microphysical scheme (rain, snow, and ice) which parameterized the dense ice species as graupel instead of hail yielded a more realistic surface rainfall distribution and radar bright band when compared against the radar data. *Adams-Selin et al*. [2013] found a greater sensitivity in accumulated precipitation to the fall speed assumption of the graupel hydrometeor class than to the number of microphysical moments alone, in agreement with *Baldauf et al*. [2011].

Varying the CRM horizontal grid size has produced sensitivities to simulated MCSs that rival those of microphysics schemes, as resolved-scale motions ultimately couple with microphysical cloud processes. Horizontal grid spacing around 4 km is required to begin resolving nonhydrostatic motions [*Weisman et al*., 1997], though subkilometer horizontal grid spacing is required to explicitly resolve most convective motions [*Bryan et al*., 2003; *Petch*, 2006]. Within this convection-permitting horizontal grid spacing range, temporally aggregated statistics such as total domain-mean precipitation show little sensitivity to grid size [*Xu and Randall*, 1995; *Weisman et al*., 1997; *Khairoutdinov and Randall*, 2001; *Lean et al*., 2008]. When examining the temporal evolution of organized convection, however, it is clear some of this insensitivity is related to compensating effects, wherein storms on a larger grid develop more slowly than storms on a finer grid, but precipitate more intensely [*Weisman et al*., 1997; BM12]. However, *Verrelle et al*. [2015] saw striking horizontal grid size sensitivities even in temporally aggregated bulk properties of thunderstorms (e.g., total surface precipitation).

A complex interplay between CRM grid spacing and microphysics has been explored in a handful of studies that vary both [*Fiori et al*., 2011; *Morrison et al*., 2015; BM12]. *Fiori et al*. [2011] performed simulations of a supercell storm across CRM grid spacing settings finding better model convergence across settings occurred with the hail-like compared to the graupel-like parameterization. *Morrison et al*. [2015] also tested sensitivities to grid spacing and microphysics, as well as environmental thermodynamic conditions, for idealized simulations of moist deep convection. They found little sensitivity in temporally aggregated bulk statistics (e.g., temporally averaged precipitation rate) to CRM grid spacing alone, but much larger sensitivities to changes in the environmental thermodynamic profile. It is therefore difficult to interpret CRM grid spacing sensitivities and determine the robustness of conclusions drawn from an idealized single-storm CRM simulation framework without understanding and sampling over the environmental conditions in which they occur.

The SP-CAM global framework with freely evolving environmental conditions provides an opportunity to sample over many large-scale conditions as they both drive and interact with convective systems. In K13, composite storm signals from internally varying ensembles of spontaneous MCS-like events over 4 month periods were intercompared. These simulations included unconstrained large-scale (up to planetary-scale) natural variability permitted by a global modeling framework. This differs significantly from the above limited-domain CRM studies, in which a single idealized MCS was simulated with various microphysical parameters or model configurations with the same initial and boundary (lateral and land-surface) conditions to minimize internal variability and convective initiation.

A key unresolved question is how detectable microphysical sensitivities are with respect to internal variability in the multiscale modeling approach. Since SP-CAM is the first GCM shown to capture the physics of mid-latitude MCSs, there are no previous modeling studies assessing the magnitude of MCS sensitivities relative to the background of global-scale variability.

Some long time series CRM experiments evaluating sensitivities to microphysics [*Wu et al*., 1999; *Liu and Moncrieff*, 2007; *Zeng et al*., 2008; *Van Weverberg et al*., 2013] and grid spacing [*VandenBerg et al*., 2014] have shown a signal above the background internal variability. Seasonal simulations of U.S. convective systems performed by *VandenBerg et al*. [2014] produced differences between test settings in phase speed and storm rotation of MCSs relative to the environment. When representing ice species as ice pellets or frozen droplets in a tropical cloud ensemble, *Wu et al*. [1999] and *Van Weverberg et al*. [2013] both observed improvements in ensemble simulations relative to observations with changes in rimed ice species parameters. Other studies suggest internal variability may dominate these sensitivities even in dynamically constrained simulations. In a 28 day evolution of central U.S. cloud ensembles, *Khairoutdinov and Randall* [2003, hereinafter KR03] found microphysical and horizontal grid spacing sensitivities of precipitation rates were within the spread of a control ensemble. While short-term CRM studies minimize the role of this internal variability by virtue of their experiment design, such sensitivities can be difficult to detect in long-term ensemble simulations, in which measuring the signal relative to background noise is a critical next step in evaluating sensitivities.

It seems reasonable to expect that model internal variability might hinder the detectability of any CRM microphysical or horizontal grid size sensitivities in seasonal ensembles of the emergent SP MCS-like signal. The null hypothesis (H1) is that CRM microphysical and horizontal grid size sensitivities in SP MCSs will not be detectable against such noise, contrary to single-storm CRM tests with controlled convective initialization. However, it is also possible that global-scale interactions and nonlocal feedbacks will amplify microphysical sensitivities, which may otherwise be constrained by initial and boundary conditions in locally confined CRM simulations, as suggested by KR03. Therefore, an alternate hypothesis (H2) is that CRM parameterization sensitivities might be greater for SP MCSs than for limited-domain CRM MCSs. If H2 is true, then we know that microphysical or grid spacing sensitivities are robust in SP-CAM.

A practical motivation of this study is to lay the groundwork for future SP GCM evaluation and tuning experiments by highlighting critical aspects of the experiment design needed for effective model development. If H2 is true, it would be most effective for modelers to leverage single-season field campaign data (which typically have the advantage of high temporal sampling from several instruments, allowing for the examination of important cloud processes in greater detail) for evaluating and tuning uncertain microphysical parameters. But if H1 is true, those advantages would be outweighed by high interannual variability, making it difficult to compare unconstrained SP GCM MCS simulations to a single season of observational data. This would argue for (1) tuning SP experiment designs against long-term observational data sets like those available through the Atmospheric Radiation Measurements (ARM) Southern Great Plains (SGP) site, and (2) focusing on multidecadal hindcasts rather than single season sensitivity studies, at the cost of added computational expense for a hindcast tuning experiment design involving a wider ensemble.

The remainder of the paper is organized into sections: section 2—describing the models, experiment design, and analysis methodology; section 3—summarizing and examining the major findings; and section 4—discussing the broader implications of this work.

2. Methods

2.1. Superparameterized Community Atmosphere Model

This experiment was performed with the SP version of CAM5 (SP-CAM5). CAM5 is the atmospheric component of the Community Earth System Model (CESM), which when run stand-alone (i.e., without fully coupled interactive ocean and sea-ice) is forced by prescribed monthly sea surface temperatures and sea ice boundary conditions. CAM5 parameterizes deep convection based on the *Zhang and McFarlane* [1995] dilute plume model and treats shallow convection with the University of Washington moist turbulence scheme [*Park and Bretherton*, 2009]. *Neale et al*. [2010] provide more details.

In contrast, SP-CAM5 replaces these convective cloud and boundary layer parameterizations with simplified (two-dimensional and laterally periodical) CRMs embedded within each latitude-longitude grid-column [*Khairoutdinov and Randall*, 2001; *Randall et al*., 2003]. That is, each independent CRM allows convection in response to large-scale GCM dynamics from CAM and returns subgrid convective heating and moistening tendencies [*Grabowski*, 2001; *Benedict and Randall*, 2009]. The approach is on the order of a 100 times more computationally expensive than conventional CAM, but scales much more efficiently on current supercomputers, [*Khairoutdinov et al*., 2005] allowing throughput capable of multidecadal climate projection. For more details about the specific version of SP-CAM used in this study, see *Wang et al*. [2011].

In this experiment, the CRMs were aligned in a north-south orientation with 28 vertical levels, which correspond to the bottom 28 levels in CAM. The exterior scale uses a finite volume dynamical core configuration at a 1.9° (latitude) by 2.5° (longitude) horizontal grid size with 30 vertical levels. The embedded CRMs have 4, 2, or 1 km horizontal grid spacing and a default column count of 32 (with the exception of one run with a 64-column grid; see section 2.3 for experiment descriptions). The time step for the embedded CRMs is 20 s while the time step for the outer-scale GCM and radiative transfer scheme is 15 min. SP-CAM5 employs a two-moment, five-class hydrometeor scheme (cloud water, cloud ice, rain, snow, and graupel) [*Morrison et al*., 2009].

2.2. MCS Identification Algorithm

The K13 MCS Index used here is based on a leading pair of empirical orthogonal function (EOF) principal component time series that identify the amplitude and phase of eastward propagating organized convective envelopes, here called "MCS-like" events. It is similar to the Madden-Julian Oscillation (MJO) Index developed by *Wheeler and Hendon* [2004], but focuses on a smaller region of zonally propagating convective activity in the central U.S. The K13 MCS Index is conditioned primarily on longwave cloud forcing (LWCF), and for this experiment was computed with an analysis region from 255°E to 275°E longitude and 36°N to 45°N latitude. As shown in K13, this approach efficiently hones in on the MCS-like storm signal in multiple years of data, providing an automated and objective method for determining MCS events in the simulations used here.

2.3. Experiment Design

To minimize the computational expense of SP simulations, only the summer season was run starting on 1 April from initial conditions spun-up in a previous CAM5 simulation. CO_2 was fixed at present-day concentrations, and sea surface temperature and sea ice concentration data were obtained from National Centers for Environmental Prediction (NCEP) Reanalysis [*Kanamitsu et al*., 2002] (see *Neale et al*. [2010] for more information on data used). We performed a total of 15 SP-CAM5 simulations, comprising 5 single-summer reference runs and 10 test runs (Table 1). Each run was simulated for 5 months starting from April, and the first month (April) was excluded from analysis as the SP-CAM5 atmosphere adjusts from CAM5 initial conditions. To represent interannual variability not forced by sea surface temperature in the SP-CAM5 reference run, CAM5 was run continuously for 6 years and the 1 April conditions from the last 5 years were used to initialize SP-CAM5 for each of the reference summers.

Table 1. Summary of Model Runs Performed[a]

Simulation Name	CRM Grid Size	Microphysical Parameters	Dense Ice Species	MCS-Like Events
Ref 0-4	2 km	Two moment	Graupel	95
2km2M[b]	2 km	Two moment	Graupel	22
Hail	2 km	Two moment	Hail	16
2km1M	2 km	One moment for rain, snow, graupel	Graupel	23
Rain	2 km	One moment for snow, graupel only	Graupel	26
Drop	2 km	Two moment; changed droplet activation	Graupel	19
Dom	2 km; 64 columns	Two moment	Graupel	23
1km2M	1 km	Two moment	Graupel	22
4km2M	4 km	Two moment	Graupel	24
1km1M	1 km	One moment for rain, snow, graupel	Graupel	32
4km1M	4 km	One moment for rain, snow, graupel	Graupel	7

[a]See section 2.3 for details.
[b]2km2M is also the same configuration of SP-CAM5 used in K13, for reference, such that results can be directly compared to that study.

Analysis of the reference run includes five 4 month periods corresponding to independent realizations of MJJA using standard microphysical settings and CRM grid spacing (two moment and 2 km, respectively). Each of the 10 test runs were initialized with an identical set of land/atmosphere initial conditions and applied physics perturbations described in Table 1 to produce an MJJA realization. For the following analysis, it is assumed that the interannual spread from the five-member ensemble reference run can be used to approximate the internal variability of the test simulations, notwithstanding differences in CRM configurations. One caveat is that the 5 year reference run is based on a slightly different version of the SP-CAM5 source code predating that used for the test runs, which is a source of potential systematic error in this analysis. The 10 test runs mimicked a set of the most robust sensitivity experiments from limited-domain CRM studies, which applied complementary configurations for simulations of a single storm or an ensemble of storms (e.g., BM12).

Most of these test runs involve modifications to CRM grid spacing, CRM microphysical formulation, or both. With 2 km, two moment as our baseline, grid size and microphysics scheme were changed in turn. Horizontal grid spacing ranged from 4, to 2, to 1 km. Microphysics tests used one-moment microphysics for various hydrometeor classes, modified the treatment of rimed ice (to represent hail instead of graupel), or modified the droplet activation.

Table 1 provides a summary of the above information, but some runs require additional explanation.

The Rain run sets snow and graupel to one-moment microphysics following the approach in *Morrison et al.* [2009], but keeps rain as two moment. This test is motivated by CRM studies that found large sensitivity to one-moment versus two-moment treatments of the rain number mixing ratio [*Morrison et al.*, 2009; *Luo et al.*, 2010; *Hong et al.*, 2010]. The 2km1M test uses a one-moment approach for rain, snow, and graupel following the approach of *Morrison et al.* [2009] and BM12.

The Hail run sets the bulk density and fall speed-size relationship of the rimed ice class to be more hail like than graupel like, following the tests in BM12. It was inspired by several studies which found striking sensitivities to the characteristics of rimed ice in modeled deep convective experiments [*McCumber et al.*, 1991; *Baldauf et al.*, 2011; *Adams-Selin et al.*, 2013; BM12].

The Drop run applies a different parameterization for droplet activation. Subgrid processes such as lateral entrainment and mixing are important in droplet activation [*Slawinska et al.*, 2012]; in most runs, the droplet activation is assumed to be dominated by these unresolved processes, and is parameterized everywhere in the cloud using a nonequilibrium supersaturation with no initial cloud water, if the diagnosed concentration of activated cloud condensation nuclei is larger than the existing droplet concentration. By contrast, the roles of unresolved entrainment and mixing in droplet activation at lateral cloud edges are ignored in the

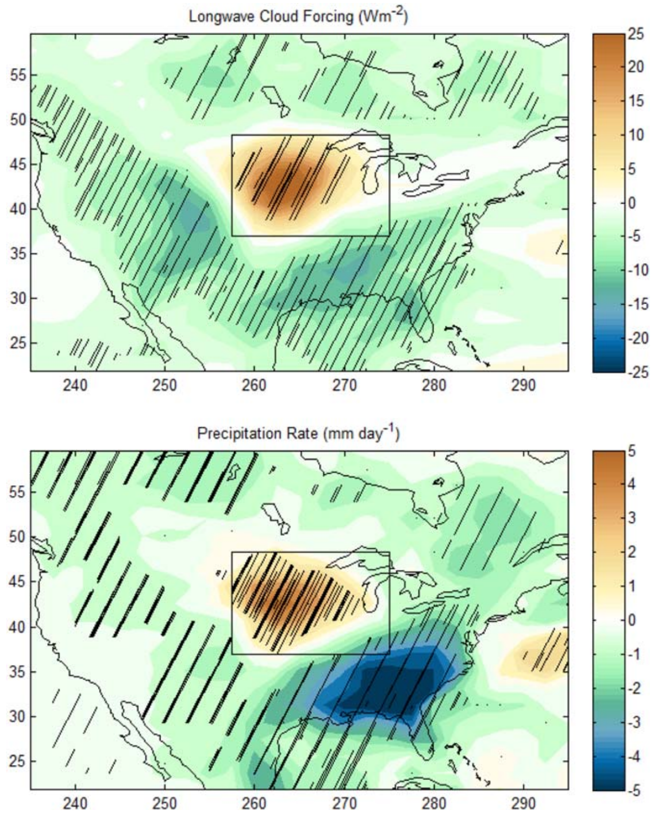

Figure 1. Nocturnal MCS-like composite anomalies (95% confidence hatched) for (top) LWCF and (bottom) precipitation rate averaged over the five-summer reference run. The inner box (i.e., analysis subregion) extends from 37°N to 48°N and 257.5°E to 275°E. Note this region is changed from the subregion on which the K13 Index was run; this particular subset of the indexed region was found to have the most consistent composite MCS-like signal, and so is used for analysis hereon. See section 2.5 for further details on map generation.

Drop simulation. Further, cloud drops in this run activate at the cloud base or in regions with little cloud water under nonequilibrium supersaturation conditions, and in the cloud interior using equilibrium supersaturation. Changing the droplet activation parameterization in turn affects droplet concentration, which has yielded interesting sensitivities. For instance, *Morrison and Grabowski* [2008] in a 2-D simulation of a rising moist thermal found a significant impact on cloud microphysical and optical properties with different assumptions of mixing and activation processes.

The Dom run tests the effects of CRM domain size independently of CRM horizontal grid spacing. Since the number of CRM columns and not the spatial extent of each CRM is controlled in most experiments, it is difficult to tease apart which sensitivities come as a result of varying grid or domain size. All other runs in this analysis have 32 CRM columns, while the Dom run has 64. In other words, the CRMs in the Dom run have a horizontal grid spacing of 2 km, but the same spatial extent of those in the 4 km runs. This simulation helps to discriminate horizontal grid size sensitivities from domain size sensitivities. Sensitivities to CRM domain size alone, through changes to the number of cloud resolving grid columns in SP-CAM, have been documented previously [*Pritchard et al.*, 2014], and highlight the importance of isolating this change independently from grid spacing.

It should be noted that prior to this analysis our computing system experienced technical issues resulting in corrupt output files, which introduced a very limited number of time gaps of 30 h increments in most of the test runs. These time gaps were filled with linear interpolation and are not expected to impact any of the major findings in this analysis.

2.4. Test Variables

To analyze summertime nocturnal MCS-like convective intensity in SP-CAM, we focus on LWCF and precipitation rate statistics. LWCF is the primary variable used in the K13 MCS Index to identify MCS propagation phase in composite anomalies. Precipitation rate is a complementary measure since it is directly related to cloud column energetics and is the primary variable analyzed in many of the limited-domain CRM microphysical and horizontal grid size sensitivity studies. Assessing it here thus allows for direct comparison to previous CRM-based findings on the response of precipitation to CRM horizontal grid size and microphysical scheme. It is worth noting though that our analysis focuses on GCM-scale sensitivities, not CRM level output, and is most directly comparable to CRM domain-mean results rather than intra-CRM-scale MCS structure. Comparing the precipitation rate response against LWCF allows us to further investigate the divergent relationship noted between them by K13, in which SP-CAM5 reduced LWCF and increased precipitation relative to SP-CAM3.5.

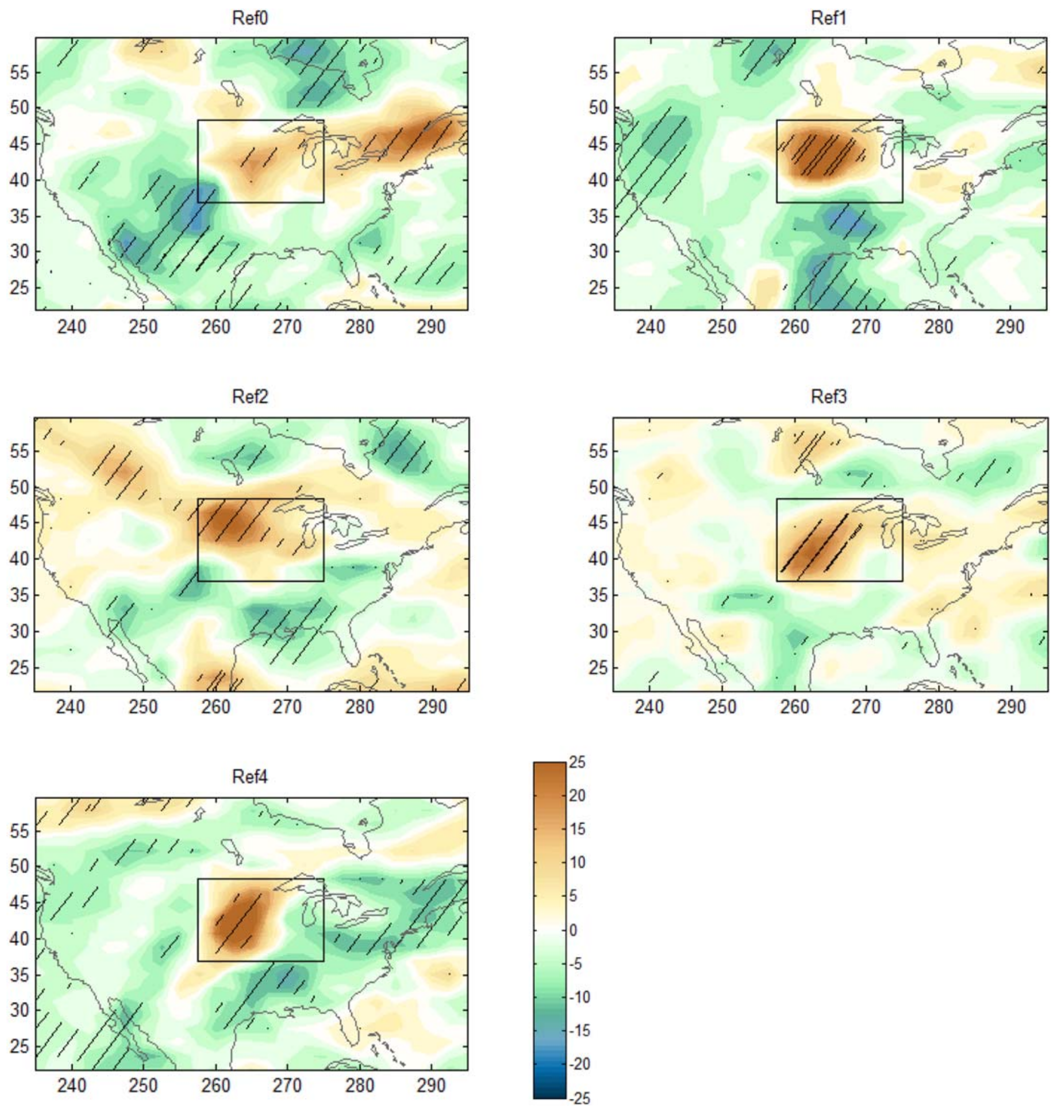

Figure 2. Nocturnal MCS-like event LWCF (W m^{-2}) composite anomalies (95% confidence hatched) for each reference summer (Ref0-4). The inner box is same as in Figure 1.

2.5. MCS Signature Verification

We ran the K13 MCS Index algorithm to objectively identify MCS-like events within the 5 year reference run. To verify a seasonal storm signal, we composited the Index-identified LWCF MCS anomalies associated with positive MCS activity during hours 6–15 UTC (local nighttime; 0–9 CST) as that diurnal phase provided a regionally consistent signal for successive years in the control run. The anomalies were computed relative to a background sample defined as summertime LWCF values in the period covering 1 week before and after each storm, during hours 6–15 UTC. That is, the control and test (MCS) samples used to define the MCS composite anomalies are seasonally and diurnally unbiased with respect to each other (i.e., controlling for the tendency of some simulations to produce storms at the beginning versus end of the summer season or at varying times of day). Since MCSs often occur sequentially, the background signal defined in this way may contain some of the MCS signal of interest, potentially reducing the magnitude of composite MCS anomalies. However, our offline analysis determined this to be the most effective approach for removing the background seasonal cycle from a single summer of data, and each simulation was processed using the same method.

All MCS composite anomalies were computed using three-hourly model output following the K13 methodology. For the purpose of defining the calibrated anomaly subregion, an unequal variances *t* test was

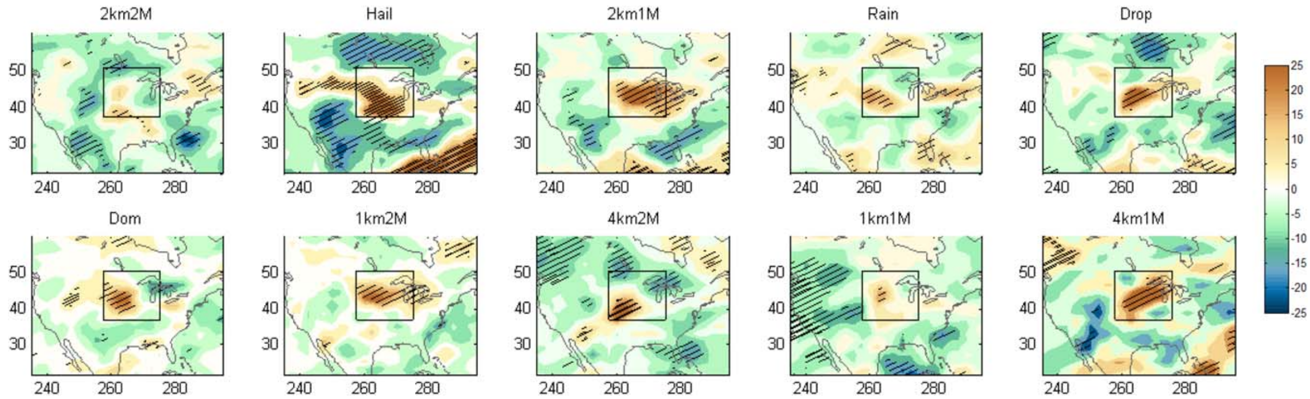

Figure 3. Nocturnal MCS-like event LWCF (W m^{-2}) composite anomalies (95% confidence hatched) for each test summer. The inner box is same as in Figure 1.

performed at each grid point within 22°N–60°N, 235°E–295°E between the test and background samples (n = 813 and 1917, respectively). Ninety-five percent confidence anomalies were used to verify identified storm activity.

Figure 1 shows the derived five-summer composite anomaly for MCS-like LWCF and precipitation from the reference run, with the analysis subregion boundaries superimposed. Figures 2 and 3 show single-summer LWCF composite anomalies for each year of the reference simulation and each of the test simulations, respectively, calculated in the same way. This confirms MCS-like events occurred in the test simulations as well as the reference simulation, as measured by LWCF and other convective intensity variables (total precipitation, ice and liquid water paths; not shown here).

2.6. Interannual and Geographic Variability

A key goal of this paper is to assess the detectability of a MCS-like event sensitivity signal in the test simulations relative to the background noise of estimated model internal interannual variability in a global climate model. Figure 2 shows the seasonal composite MCS-like event LWCF anomaly in each of the five independent years from the reference run. Clearly, there is significant interannual variability in the MCS-like event signal intensity, with reference year 0 (Ref0) having approximately half the intensity of the following year (Ref1; see Figure 2). Qualitatively, the amount of internal variability appears to rival the test run sensitivities with varied microphysics setup and CRM horizontal grid spacing in Figure 3.

2.7. Dynamic Sampling of Individual Storms

The boxed subregion shown in Figures 1–3 encompasses a larger spatial extent than any individual storm. It was decided from here that a seasonal composite analysis may obscure the full magnitude of any MCS-like event LWCF or precipitation rate signals by convolving them with non-MCS signals in the boxed subregion. While using a large spatial extent relative to individual storm size might allow us to harmonize the area of interest across runs which display considerable geographic variation of storms from one another (Figure 2), it might also introduce the potential for additional geographic noise.

To offset this, we manually calibrated the distinct action centers of individual MCSs as initially identified by the K13 MCS identification algorithm. Both a central horizontal location and time were recorded for the maximum of each nocturnal storm. To minimize geographic noise, each storm sample was defined first as a mean intensity accumulated from plus or minus one latitude grid point (±1.9°N) and four longitude grid points (±10°E) from the manually identified central horizontal location, and plus or minus eight three-hourly time samples (±24 h) from the identified storm temporal maximum.

Figure 4 shows Hovmoller diagrams of MCS events from one summer of the reference simulation (Ref4, which had the highest number of events in the five-summer reference run), and confirms that most events had a spatiotemporal evolution matching the expected eastward propagation.

An intensity signal for each storm was achieved via an objective line-fitting algorithm, which tracked only the strongest positive propagating LWCF signal associated with each storm. To form an anomaly signal, a background sample was subtracted from this test sample. The background sample for each storm was

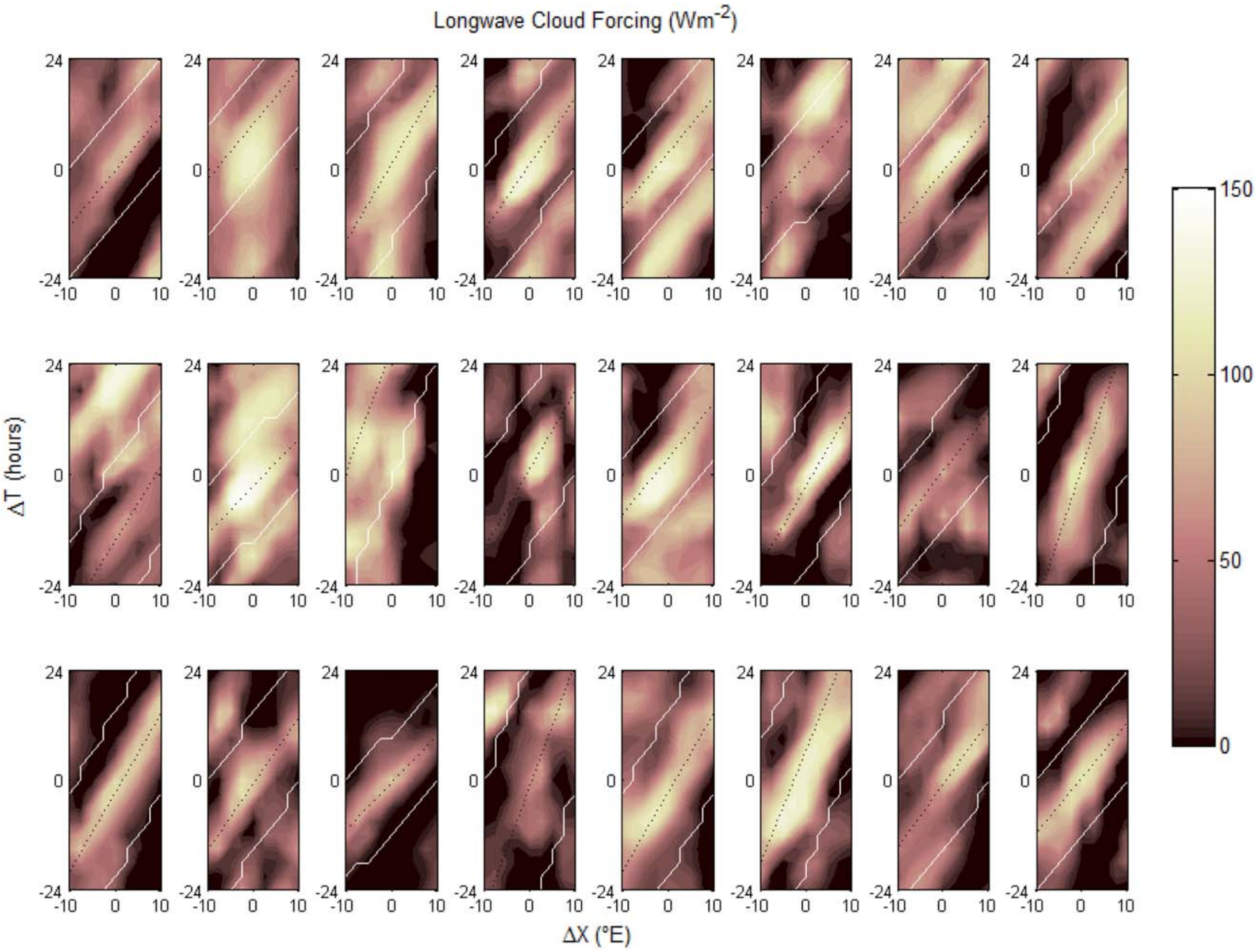

Figure 4. Ref4 individual MCS-like storm event LWCF across longitude and time. All values were averaged first over three latitude grid points (±1.9°N from recorded storm maximum latitude). The zeroth hour differs for each event and was defined manually as the storm maximum time, i.e., storms are not temporally harmonized with respect to one another, in contrast with the analyses shown in Figures 2 and 3. The black dotted line is the best fit line and the white solid lines are the boundaries used for sampling (such that any values outside of the white lines were not included in the test samples) as determined by the line-fitting algorithm.

defined with the same spatial extent as the test sample (±1.9° and ±10°E from the recorded storm maximum), but temporally as including all times from 1 week before to 1 week after the recorded storm center. In other words, the analysis was performed on a storm-by-storm basis where the test and control samples were geographically and seasonally unbiased with respect to one another for each individual storm event. This technique allows a more surgical approach in which regions of MCS activity were pinpointed for each storm, and thus minimally influenced by simultaneous, unrelated background signals.

To create a compact aggregate intensity statistic, each storm sample had its corresponding background sample subtracted from it; all these storm-scale anomalies were then horizontally averaged over the season (Figure 5; circles). The standard error (error bars on Figure 5; see equation (1)) was then calculated across the anomalies within each season; the error bars therefore represent the intraseasonal (storm-to-storm) variability within each run. A standard error was also calculated across all five reference years to represent the interannual variability (shading on Figure 5) and provide a baseline against which to evaluate potential sensitivities between our single-summer test runs.

Note that the same spatiotemporal envelope developed for LWCF streaks in Figure 4 (envelope edges outlined in white) was used on precipitation rate to maintain sample size consistency between variables despite some differences in the spatial extent of the region with nonzero precipitation rate, which tended to have a more geographically confined signal than LWCF.

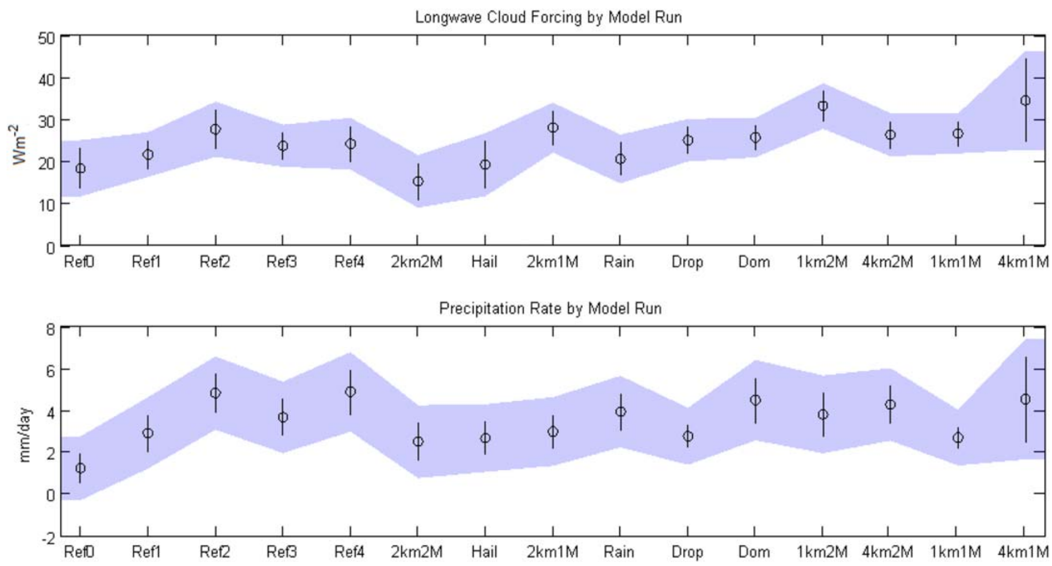

Figure 5. Horizontal means (circles) and horizontal standard errors (bars) and 5 year reference interannual spread (shading; added onto bars to better show interannual variability) of the MCS-like storm-level composite anomalies. Error bars represent the standard error (see equation (1)) over all the storm anomalies (individual storm minus its corresponding background sample) in the summer. Shading is the standard error across all storm anomalies in the 5 year reference run.

3. Results and Discussion

3.1. Microphysical Sensitivities

Our main finding is that MCS-like sensitivities are mostly indistinguishable from large interannual and intraseasonal variability (Figure 5). This adds a new dimension to what is found in complementary experiments in a limited-domain CRM test-harness when convective initiation is constrained by the initialization procedure (e.g., BM12) and suggests that internal variability is larger in SP-CAM, making sensitivities harder to detect.

3.2. Implications for Signal Detectability

Our results suggest that enhanced sampling is likely needed to detect MCS microphysical sensitivities in seasonal SP-CAM simulations. It is natural to wonder how much added sampling would be needed based on the level of internal variability in SP-CAM's MCS-like signal that we have found. That is, assuming the intraseasonal variability over our 5 year reference run is a reliable estimate of SP-CAM MCS-like storm internal variability, we can calculate how many individual SP-CAM MCS-like storms would need to be sampled in order to detect a robust sensitivity, which may help inform future hindcast experiment design.

As a thought experiment, we will examine this question under the assumption that the true amplitude of microphysical sensitivities is known from CRM studies with initialized convection—a reasonable first estimate, albeit excluding nonlocal feedback. At the CRM-domain mean scale of $O(150\text{ km} \times 400\text{ km} \times 3\text{ h})$, a characteristic amplitude is $\sim$5 mm/d, the response to varying order of microphysics for a midlatitude squall line found by BM12. To sample SP-CAM's MCS-like signal at a similar spatiotemporal scale, we redefine an intensity signal for each storm as the maximum precipitation rate value per storm such that the sampling for each storm occurs at a scale of one 3 h averaging interval, and a single horizontal grid point (1.9° latitude by 2.5° longitude). This brings us close to the spatial and temporal scales of the BM12 CRM model setup, allowing a fair comparison between CRM microphysical sensitivity amplitude and SP-CAM internal MCS-like storm variability.

To estimate the number of samples that would be needed to detect sensitivities of SP-CAM's MCS-like organized storm events at 95% confidence for a sensitivity of this magnitude, we consider the requirement that the signal's sensitivity magnitude Y exceed twice its standard error SE,

$$2\ \text{SE} \approx \frac{2\sigma}{\sqrt{N-1}} < Y, \tag{1}$$

where σ is the standard deviation of the MCS signal and N is the number of MCS events sampled. We solve equation (1) for N, assuming a precipitation signal magnitude of $Y \sim 5$ mm/d from BM12, and calculating

Table 2. Estimated Number of Samples Needed to Detect Robust MCS Sensitivities Comparable to BM12

Test	Y (From BM12; mm/d)	N >	Approximate # Summers
2M–1M microphysics (1 km grid)	−5.7870	105	5 ± 2
2M–1M microphysics (4 km grid)	0.9645	3750	179 ± 40
4 km–1 km grid (1M)	−8.6806	47	3 ± 2
4 km–1 km grid (2M)	−1.9290	938	45 ± 10

the standard deviation σ from our 5 year reference run, which encompasses the variability in storm precipitation anomalies across 95 total events over five seasons (we find $\sigma = 29.5$ mm/d).

This yields an estimate of the storm sample sizes that would be needed to detect microphysical sensitivities at 95% significance. The results are summarized in Table 2, which illustrates that ensembles of at least 100 storms (i.e., at least five seasons) are likely required to detect microphysical sensitivities, given the high internal variability in SP-CAM's MCS-like storm signal.

3.3. Experiment Design Disparities

We have found that microphysical sensitivities are not large enough in SP-CAM MCS-like event simulations to be robustly detectable amidst high internal variability in single-season simulations. In some ways, this could be viewed as hard to reconcile with CRM studies that have shown striking microphysical MCS sensitivities under more controlled conditions. In other ways, it is perhaps unsurprising, given that convective triggering and initiation is highly internally variable in SP-CAM simulations (Table 1), and the interactive global framework introduces many more degrees of freedom. Having quantified this internal variability, it is clear that greater storm sampling (>100 member ensemble) may be required to analyze the microphysical sensitivities of SP-CAM's MCS-like event signal, and that previous findings about the current fidelity of this signal contain sampling uncertainty.

Several other important differences between this SP-CAM study and previous CRM work are worth acknowledging. First, it is not clear how vertical resolution differences between limited-domain CRM studies and our study may have impacted the results, which makes direct comparison difficult. A typical shortcoming of SP-GCMs is a coarse vertical resolution that is inherited from the host GCM and which makes the simulations computationally viable. Since sensitivities have been found in convection to the vertical resolution of the model used [*Khairoutdinov et al*., 2009], it must be acknowledged that the coarse vertical CRM grid may have impacted the results in a way that obscures direct comparison with much of the CRM sensitivity literature. It is possible higher vertical resolution may make SP-GCMs more sensitive to microphysical and horizontal grid size changes, but that remains to be seen.

It is natural to wonder if the limited dimensionality of the CRMs in SP-CAM could likewise affect the outcome of sensitivity tests. Dimensionality sensitivity tests have been performed on simulations of organized convection [*Grabowski et al*., 1998; *Tompkins*, 2000; *Xu et al*., 2002; *Petch*, 2006; *Zeng et al*., 2008], which suggest bulk statistics from two-dimensional simulations are in some cases comparable to three-dimensional simulations. *Zeng et al*. [2008] observed a complex interplay between CRM dimensionality and microphysics sensitivities, in which ensembles with higher ice nuclei concentrations exhibited a greater sensitivity to dimensionality in terms of time-varying precipitation rates and cloud hydrometeor profiles; however, time-mean precipitation rates were largely insensitive to dimensionality. That said, not all results agree with this conclusion. For instance, *Phillips and Donner* [2006] found significant differences even in bulk statistics (e.g., vertical mass fluxes) between two-dimensional and three-dimensional domains, and in turn found an influence between dimensionality and microphysics. Additionally, *Weisman et al*. [1997] found key differences in the horizontal grid size sensitivities of a simulated squall line between two-dimensional and three-dimensional domains. Thus, it is unclear whether the limited dimensionality of SP-CAM's CRMs influenced the sensitivities seen here. However, as stressed earlier, the two-dimensional physics of the inner CRMs in SP-CAM do not operate independently of the three-dimensional dynamics on the GCM scale, and diagnosing the influence of CRM dimensionality is not as straightforward as it is in a conventional CRM framework.

When comparing CRM MCSs to SP-CAM MCS features, it is necessary to acknowledge spatiotemporal-scale differences between the two frameworks. That is to say, while SP-CAM has embedded CRMs, all data analyzed here were averaged over the GCM grid in which the CRM column resided—potentially masking differences that may emerge as finer CRM-scale sensitivities. Without independently assessing

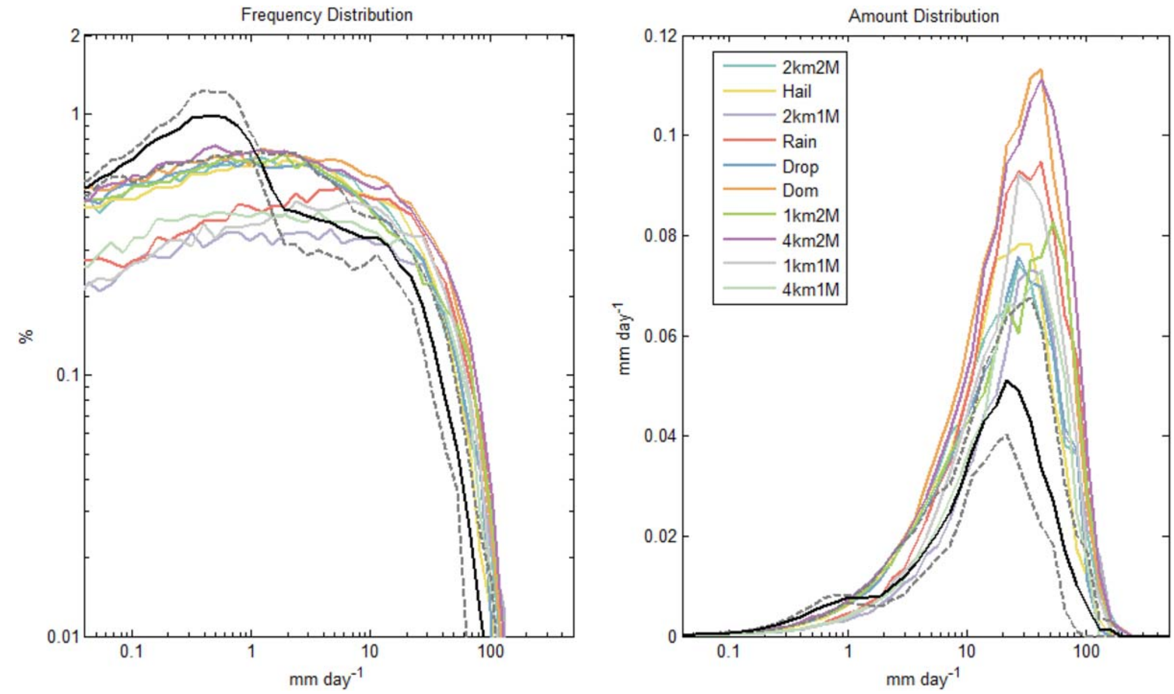

Figure 6. (left) Frequency and (right) amount distributions (normalized by logarithmically spaced precipitation bins) for seasonal rainfall from 37°N to 48°N and 250°E to 275°E. Note the slightly larger domain compared to the MCS analysis; it was extended further westward to include the stable rainfall region east of the Rockies. The dashed lines represent the interannual spread from the five-summer reference run, while the solid black line is the mean for all five summers.

CRM-level output within each model run, it is difficult to estimate the magnitude of sensitivities on this inner scale.

Finally, another potential issue inherent to our methodology is the exclusive use of the K13 MCS Index algorithm to identify MCS events. While K13 did show a promising storm signal as identified by the Index, and storms within this analysis were manually verified to be consistent with expectations, there still exists the possibility for bias. For example, the nature of the K13 Index may have favored only certain types of convection (e.g., large, eastward propagating storms), thereby limiting our sample size. It is a challenge to reliably identify mesoscale storms in SP GCMs, and it is possible that a different, more inclusive MCS identification algorithm could have yielded different results.

3.4. Precipitation Unconditioned on the U.S. MCS Index

To address the last concern, we separately analyze overall (seasonal-domain mean) rainfall statistics independently from the K13 MCS Index. Figure 6 shows MJJA (left) rainfall frequency and (right) amount distributions for the reference and test runs within the boxed subregion (from Figures 1–3) extended slightly more to the west (250°E) to illustrate the seasonal variability in precipitation intensity. Figure 6 demonstrates that, independent of the K13 MCS Index, there is a large amount of interannual variability in the reference simulation, especially in terms of total seasonal precipitation amount (integral of the amount distribution in Figure 6). Though the total amount of rainfall varies somewhat across test simulations, the general shape (intensity) of the amount distribution in Figure 6 is fairly insensitive and within the range of variability from the reference simulation. The most compelling potential sensitivity appears to be a bifurcation in the frequency of lower rain rates in Figure 6, but this contributes little to the accumulated rainfall amount and is not likely to be associated with high-intensity MCS events. Though this is only one measure of bulk precipitation sensitivity, it supports the earlier result that internal variability is larger than the microphysical sensitivities regardless of whether the analysis is conditioned on an MCS Index.

4. Conclusions

Superparameterized GCMs, characterized by *O*(1–4 km) CRMs embedded in each grid column of a host GCM, offer opportunities for studying sensitivities of mesoscale convection without sacrificing global feedbacks and realistic large-scale variability. However, SP-GCMs are in their infancy and the MCS-like signal they simulate is a fledgling one. Since inconsistencies in the realism of composite MCS storm signals have been documented between recent SP-CAM model versions (K13), it is clear that a greater understanding of CRM grid spacing and microphysics formulation sensitivities is necessary.

The advantage of MCS sensitivity studies using SP-GCMs including complex weather-climate interactions comes at the cost of introducing model internal variability that is avoided by preventing feedbacks between the large and convective scales in the classic, limited-domain CRM-based studies. While this can limit the detectability of MCS sensitivities in SP-GCMs, it also could be viewed as a useful bridge for assessing whether those sensitivities seen under controlled conditions manifest comparably at larger scales, or are potentially even amplified or damped through nonlocal feedbacks. That is, multimonth simulations with SP-GCMs provide an interesting complementary framework for studying MCSs: without periodic lateral boundaries or memory of harmonized initial conditions, SP-CAM MCS-like storm events form spontaneously.

This study aimed to do the following: (1) characterize MCS-like interannual variability in SP-CAM to provide a sufficient background spread against which any sensitivities could be verified, (2) test whether microphysical assumptions and CRM horizontal grid size produce detectable effects on MCS-like activity at the seasonal scale beyond this variability, and (3) use these results to better inform the future experiment design and use of observational data in tuning unconstrained microphysical parameters to optimize the fledgling MCS-like event signal in SP-GCMs. We began with a five-summer reference simulation run under a particular set of fixed conditions (2 km horizontal grid spacing, two-moment microphysics) to generally estimate MCS-like event internal variability in SP-CAM5. We followed this with 10 single-summer SP-CAM5 runs, varying microphysics and CRM grid spacing setups as inspired by literature on CRM-based MCS sensitivities (see Table 1 for details). A MCS identification algorithm developed by K13 conditioned on LWCF and characteristic MCS eastward propagation was applied over the central U.S. to identify individual storms. We focused on two measures of convective intensity: LWCF and precipitation rate. Amidst high geographic noise, we performed a surgical analysis in which individual storms were singled out by excluding nonstorm activity as determined by a LWCF threshold value (Figure 4).

The main finding is that the sensitivities of SPCAM's MCS-like storms in LWCF and precipitation rate were not statistically detectable from large internal variability (Figure 5). This indicates that there exists greater dispersion from interannual and inter-storm variability than from CRM microphysics parameterizations and horizontal grid spacing, at least in the context of single-summer ensembles of SP MCS-like events. In hindsight, these results imply that it is unknowable whether CRM microphysics parameterization updates from SP-CAM3/3.5 to 5 actually resulted in the more realistic MCS-like LWCF and precipitation rate signals as hypothesized in K13; thus, H1, the null hypothesis that these changes occurred entirely due to chance, cannot be ruled out.

Our results argue against the use of single-summer SP-CAM runs to attempt to document SP MCS-like storm sensitivities, since interannual variability of the signal is so high; instead, multiseason, potentially multidecadal, test runs may be necessary to tease apart sensitivities from the background internal spread. Accordingly, it is unknown whether the use of two-moment microphysics or CRM horizontal grid spacing finer than 4 km have produced performance increases for the MCS signal in single-summer SP-CAM5 runs relative to earlier versions, or whether the performance increases themselves were robustly detected. Future work will explore whether sensitivities are detectable in targeted, longer multiseason runs. Based on the internal variability quantified in our analysis, we have identified that an ensemble size of at least a hundred independent storms—5 times more than were sampled in this study—will be needed to detect MCS sensitivities.

The finding of insensitivity relative to internal variability may argue against an idea set forth in KR03, where it was speculated that the inclusion of nonlocal feedbacks to intra-CRM microphysical sensitivities could serve to amplify them amidst noise that otherwise overwhelm them over long time scales, large spatial domains, and multiple interacting cloud systems. Instead, it appears the global feedbacks facilitated by SP have led to internal variability of MCS intensity that is much stronger than its sensitivity to microphysical and grid configuration variations, at least at the 4 month time scale.

Finally, our results have some practical implications for designing future experiments to tune the microphysical properties of MCS-like signals in SP GCMs, assuming they are indeed tunable despite intrinsic approximations at the CRM scale. Based on the sampling requirements, SP GCM storm tuning may especially benefit from the inclusion of multidecadal cloud statistics such as those available through the ARM SGP site in addition to the higher-resolution and more frequently sampled data available through seasonally limited field campaigns (e.g., ARM's Midlatitude Continental Convective Cloud Experiment) [*Williams*, 2012; *Tridon et al*., 2013]. Hindcast tuning testbeds that seek to optimize SP-CAM's MCS signal will likely need to sample more than five seasons or over 100 storms of observed activity to constrain and improve its realism. Successful tuning is in turn a necessary task for future climate sensitivity applications of superparameterized climate simulation technology focusing on the central U.S. MCS—a global climate change nexus, where it currently has unique potential.

Acknowledgments
The authors would like to thank the Editor and two anonymous reviewers for constructive comments that helped improve the manuscript. All model results and code used to produce the figures in this paper are archived at UC Irvine and available on request. All test model runs were performed by Jack Ritchie and John Helly. We would like to thank the U.S. Department of Energy Office of Science and Research for providing funding under award DE-SC0012152. Gabriel Kooperman acknowledges support from a National Science Foundation Postdoctoral Research Fellowship under award AGS-1349579.

References

Adams-Selin, R. D., S. C. van den Heever, and R. H. Johnson (2013), Sensitivity of bow-echo simulation to microphysical parameterizations, *Weather Forecasting*, *28*(5), 1188–1209, doi:10.1175/WAF-D-12-00108.1.

Bacmeister, J. T., M. F. Wehner, R. B. Neale, A. Gettelman, C. Hannay, P. H. Lauritzen, J. M. Caron, and J. E. Truesdale (2014), Exploratory high-resolution climate simulations using the Community Atmosphere Model (CAM), *J. Clim.*, *27*, 3073–3099, doi:10.1175/JCLI-D-13-00387.1.

Baldauf, M., A. Seifert, J. Förstner, D. Majewski, M. Raschendorfer, and T. Reinhardt (2011), Operational convective-scale numerical weather prediction with the COSMO model: Description and sensitivities, *Mon. Weather Rev.*, *139*(12), 3887–3905.

Benedict, J. J., and D. A. Randall (2009), Structure of the Madden–Julian Oscillation in the superparameterized CAM, *J. Atmos. Sci.*, *66*, 3277–3296.

Bryan, G. H., and H. Morrison (2012), Sensitivity of a simulated squall line to horizontal resolution and parameterization of microphysics, *Mon. Weather Rev.*, *140*(1), 202–225.

Bryan, G. H., J. C. Wyngaard, and J. M. Fritsch (2003), Resolution requirements for the simulation of deep moist convection, *Mon. Weather Rev.*, *131*(10), 2394–2416, doi:10.1175/1520-0493(2003)131<2394:RRFTSO>2.0.CO;2.

Dawson, D. T., M. Xue, J. A. Milbrandt, and M. K. Yau (2010), Comparison of evaporation and cold pool development between single-moment and multimoment bulk microphysics schemes in idealized simulations of tornadic thunderstorms, *Mon. Weather Rev.*, *138*(4), 1152–1171, doi:10.1175/2009MWR2956.1.

Fiori, E., A. Parodi, and F. Siccardi (2011), Uncertainty in prediction of deep moist convective processes: Turbulence parameterizations, microphysics and grid-scale effects, *Atmos. Res.*, *100*(4), 447–456, doi:10.1016/j.atmosres.2010.10.003.

Fovell, R. G., and Y. Ogura (1988), Numerical Simulation of a Midlatitude Squall Line in Two Dimensions, *J. Atmos. Sci.*, *45*(24), 3846–3879, doi:10.1175/1520-0469(1988)045<3846:NSOAMS>2.0.CO;2.

Gilmore, M. S., J. M. Straka, and E. N. Rasmussen (2004), Precipitation uncertainty due to variations in precipitation particle parameters within a simple microphysics scheme, *Mon. Weather Rev.*, *132*(11), 2610–2627, doi:10.1175/MWR2810.1.

Grabowski, W. W. (2001), Coupling cloud processes with the large-scale dynamics using the Cloud-Resolving Convection Parameterization (CRCP), *J. Atmos. Sci.*, *58*(9), 978–997, doi:10.1175/1520-0469(2001)058<0978:CCPWTL>2.0.CO;2.

Grabowski, W. W., X. Wu, M. W. Moncrieff, and W. D. Hall (1998), Cloud-resolving modeling of cloud systems during phase III of GATE. Part II: Effects of resolution and the third spatial dimension, *J. Atmos. Sci.*, *55*(21), 3264–3282.

Hong, S.-Y., K.-S. S. Lim, Y.-H. Lee, J.-C. Ha, H.-W. Kim, S.-J. Ham, and J. Dudhia (2010), Evaluation of the WRF double-moment 6-class microphysics scheme for precipitating convection, *Adv. Meteorol.*, *2010*, 10 pp., doi:10.1155/2010/707253.

Igel, A. L., M. R. Igel, and S. C. van den Heever (2014), Make it a double? Sobering results from simulations using single-moment microphysics schemes, *J. Atmos. Sci.*, *72*(2), 910–925, doi:10.1175/JAS-D-14-0107.1.

Kanamitsu, M., W. Ebisuzaki, J. Woollen, S.-K. Yang, J. J. Hnilo, M. Fiorino, and G. L. Potter (2002), NCEP–DOE AMIP-II Reanalysis (R-2), *Bull. Am. Meteorol. Soc.*, *83*(11), 1631–1643, doi:10.1175/BAMS-83-11-1631.

Khairoutdinov, M., D. Randall, and C. DeMott (2005), Simulations of the atmospheric general circulation using a cloud-resolving model as a superparameterization of physical processes, *J. Atmos. Sci.*, *62*(7), 2136–2154, doi:10.1175/JAS3453.1.

Khairoutdinov, M. F., and D. A. Randall (2001), A cloud resolving model as a cloud parameterization in the NCAR Community Climate System Model: Preliminary results, *Geophys. Res. Lett.*, *28*(18), 3617–3620, doi:10.1029/2001GL013552.

Khairoutdinov, M. F., and D. A. Randall (2003), Cloud resolving modeling of the ARM summer 1997 IOP: Model formulation, results, uncertainties, and sensitivities, *J. Atmos. Sci.*, *60*(4), 607–625, doi:10.1175/1520-0469(2003)060<0607:CRMOTA>2.0.CO;2.

Khairoutdinov, M. F., S. K. Krueger, C.-H. Moeng, P. A. Bogenschutz, and D. A. Randall (2009), Large-eddy simulation of maritime deep tropical convection, *J. Adv. Model. Earth Syst.*, *1*, 15, doi:10.3894/JAMES.2009.1.15.

Kooperman, G. J., M. S. Pritchard, and R. C. J. Somerville (2013), Robustness and sensitivities of central U.S. summer convection in the super-parameterized CAM: Multi-model intercomparison with a new regional EOF index, *Geophys. Res. Lett.*, *40*, 3287–3291, doi:10.1002/grl.50597.

Lean, H. W., P. A. Clark, M. Dixon, N. M. Roberts, A. Fitch, R. Forbes, and C. Halliwell (2008), Characteristics of high-resolution versions of the Met Office unified model for forecasting convection over the United Kingdom, *Mon. Weather Rev.*, *136*(9), 3408–3424, doi:10.1175/2008MWR2332.1.

Liu, C., and M. W. Moncrieff (2007), Sensitivity of cloud-resolving simulations of warm-season convection to cloud microphysics parameterizations, *Mon. Weather Rev.*, *135*(8), 2854–2868, doi:10.1175/MWR3437.1.

Luo, Y., Y. Wang, H. Wang, Y. Zheng, and H. Morrison (2010), Modeling convective-stratiform precipitation processes on a Mei-Yu front with the Weather Research and Forecasting model: Comparison with observations and sensitivity to cloud microphysics parameterizations, *J. Geophys. Res.*, *115*, D18117, doi:10.1029/2010JD013873.

McCumber, M., W.-K. Tao, J. Simpson, R. Penc, and S.-T. Soong (1991), Comparison of ice-phase microphysical parameterization schemes using numerical simulations of tropical convection, *J. Appl. Meteorol. Climatol.*, *30*(7), 985–1004, doi:10.1175/1520-0450-30.7.985.

Meyers, M. P., R. L. Walko, J. Y. Harrington, and W. R. Cotton (1997), New RAMS cloud microphysics parameterization. Part II: The two-moment scheme, *Atmos. Res.*, *45*(1), 3–39, doi:10.1016/S0169-8095(97)00018-5.

Milbrandt, J. A., and M. K. Yau (2005), A multimoment bulk microphysics parameterization. Part II: A proposed three-moment closure and scheme description, *J. Atmos. Sci.*, *62*(9), 3065–3081, doi:10.1175/JAS3535.1.

Moncrieff, M. W., and C. Liu (2006), Representing convective organization in prediction models by a hybrid strategy, *J. Atmos. Sci.*, *63*(12), 3404–3420, doi:10.1175/JAS3812.1.

Morrison, H., and W. W. Grabowski (2008), Modeling supersaturation and subgrid-scale mixing with two-moment bulk warm microphysics, *J. Atmos. Sci.*, *65*(3), 792–812, doi:10.1175/2007JAS2374.1.

Morrison, H., J. A. Curry, and V. I. Khvorostyanov (2005), A new double-moment microphysics parameterization for application in cloud and climate models. Part I: Description, *J. Atmos. Sci.*, *62*(6), 1665–1677, doi:10.1175/JAS3446.1.

Morrison, H., G. Thompson, and V. Tatarskii (2009), Impact of cloud microphysics on the development of trailing stratiform precipitation in a simulated squall line: Comparison of one- and two-moment schemes, *Mon. Weather Rev.*, *137*(3), 991–1007, doi:10.1175/2008MWR2556.1.

Morrison, H., A. Morales, and C. Villanueva-Birriel (2015), Concurrent sensitivities of an idealized deep convective storm to parameterization of microphysics, horizontal grid resolution, and environmental static stability, *Mon. Weather Rev.*, *143*(6), 2082–2104, doi:10.1175/MWR-D-14-00271.1.

Neale, R. B., et al. (2010), Description of the NCAR Community Atmosphere Model (CAM 5.0), NCAR Technical Note, Natl. Cent. for Atmos. Res., Boulder, Colo.

Nicholls, M. E., and M. J. Weissbluth (1988), A comparison of two-dimensional and quasi-three-dimensional simulations of a tropical squall line, *Mon. Weather Rev.*, *116*(12), 2437–2452, doi:10.1175/1520-0493(1988)116<2437:ACOTDA>2.0.CO;2.

Park, S., and C. S. Bretherton (2009), The University of Washington shallow convection and moist turbulence schemes and their impact on climate simulations with the Community Atmosphere Model, *J. Clim.*, *22*(12), 3449–3469, doi:10.1175/2008JCLI2557.1.

Petch, J. C. (2006), Sensitivity studies of developing convection in a cloud-resolving model, *Q. J. R. Meteorol. Soc.*, *132*(615), 345–358, doi:10.1256/qj.05.71.

Phillips, V. T. J., and L. J. Donner (2006), Cloud microphysics, radiation and vertical velocities in two- and three-dimensional simulations of deep convection, *Q. J. R. Meteorol. Soc.*, *132*(621C), 3011–3033, doi:10.1256/qj.05.171.

Pritchard, M. S., M. W. Moncrieff, and R. C. J. Somerville (2011), Orogenic propagating precipitation systems over the United States in a global climate model with embedded explicit convection, *J. Atmos. Sci.*, *68*(8), 1821–1840, doi:10.1175/2011JAS3699.1.

Pritchard, M. S., C. S. Bretherton, and C. A. DeMott (2014), Restricting 32-128 km horizontal scales hardly affects the MJO in the Superparameterized Community Atmosphere Model v.3.0 but the number of cloud-resolving grid columns constrains vertical mixing, *J. Adv. Model. Earth Syst.*, *6*(3), 723–739, doi:10.1002/2014MS000340.

Randall, D., M. Khairoutdinov, A. Arakawa, and W. Grabowski (2003), Breaking the cloud parameterization deadlock, *Bull. Am. Meteorol. Soc.*, *84*(11), 1547–1564, doi:10.1175/BAMS-84-11-1547.

Schlesinger, R. E. (1984), Effects of the pressure perturbation field in numerical models of unidirectionally sheared thunderstorm convection—Two versus three dimensions, *41*(9), 1571–1587.

Seifert, A., and K. D. Beheng (2001), A double-moment parameterization for simulating autoconversion, accretion and selfcollection, *Atmos. Res.*, *59-60*, 265–281, doi:10.1016/S0169-8095(01)00126-0.

Slawinska, J., W. W. Grabowski, H. Pawlowska, and H. Morrison (2012), Droplet activation and mixing in large-eddy simulation of a shallow cumulus field, *J. Atmos. Sci.*, *69*(2), 444–462, doi:10.1175/JAS-D-11-054.1.

Tompkins, A. M. (2000), The impact of dimensionality on long-term cloud-resolving model simulations, *Mon. Weather Rev.*, *128*(5), 1521–1535, doi:10.1175/1520-0493(2000)128<1521:TIODOL>2.0.CO;2.

Tridon, F., A. Battaglia, P. Kollias, E. Luke, and C. R. Williams (2013), Signal postprocessing and reflectivity calibration of the atmospheric radiation measurement program 915-MHz wind profilers, *J. Atmos. Oceanic Technol.*, *30*(6), 1038–1054, doi:10.1175/JTECH-D-12-00146.1.

VandenBerg, M. A., M. C. Coniglio, and A. J. Clark (2014), Comparison of next-day convection-allowing forecasts of storm motion on 1- and 4-km Grids, *Weather Forecasting*, *29*(4), 878–893, doi:10.1175/WAF-D-14-00011.1.

Van Weverberg, K., A. M. Vogelmann, H. Morrison, and J. A. Milbrandt (2012), Sensitivity of idealized squall-line simulations to the level of complexity used in two-moment bulk microphysics schemes, *Mon. Weather Rev.*, *140*(6), 1883–1907, doi:10.1175/MWR-D-11-00120.1.

Van Weverberg, K., A. M. Vogelmann, W. Lin, E. P. Luke, A. Cialella, P. Minnis, M. Khaiyer, E. R. Boer, and M. P. Jensen (2013), The role of cloud microphysics parameterization in the simulation of mesoscale convective system clouds and precipitation in the tropical western Pacific, *J. Atmos. Sci.*, *70*(4), 1104–1128.

Verrelle, A., D. Ricard, and C. Lac (2015), Sensitivity of high-resolution idealized simulations of thunderstorms to horizontal resolution and turbulence parametrization, *Q. J. R. Meteorol. Soc.*, *141*(687), 433–448, doi:10.1002/qj.2363.

Wandishin, M. S., D. J. Stensrud, S. L. Mullen, and L. J. Wicker (2008), On the predictability of mesoscale convective systems: Two-dimensional simulations, *Weather Forecasting*, *23*(5), 773–785, doi:10.1175/2008WAF2007057.1.

Wandishin, M. S., D. J. Stensrud, S. L. Mullen, and L. J. Wicker (2010), On the predictability of mesoscale convective systems: Three-dimensional simulations, *Mon. Weather Rev.*, *138*(3), 863–885, doi:10.1175/2009MWR2961.1.

Wang, M., et al. (2011), The multi-scale aerosol-climate model PNNL-MMF: Model description and evaluation, *Geosci. Model Dev.*, *4*(1), 137–168, doi:10.5194/gmd-4-137-2011.

Weisman, M. L., J. B. Klemp, and R. Rotunno (1988), Structure and evolution of numerically simulated squall lines, *J. Atmos. Sci.*, *45*(14), 1990–2013, doi:10.1175/1520-0469(1988)045<1990:SAEONS>2.0.CO;2.

Weisman, M. L., W. C. Skamarock, and J. B. Klemp (1997), The resolution dependence of explicitly modeled convective systems, *Mon. Weather Rev.*, *125*(4), 527–548, doi:10.1175/1520-0493(1997)125<0527:TRDOEM>2.0.CO;2.

Wheeler, M. C., and H. H. Hendon (2004), An all-season real-time multivariate MJO index: Development of an Index for Monitoring and Prediction, Mon. *Weather Rev.*, *132*(8), 1917–1932, doi:10.1175/1520-0493(2004)132<1917:AARMMI>2.0.CO;2.

Williams, C. R. (2012), Vertical air motion retrieved from dual-frequency profiler observations, *J. Atmos. Oceanic Technol.*, *29*(10), 1471–1480, doi:10.1175/JTECH-D-11-00176.1.

Wu, X., W. D. Hall, W. W. Grabowski, M. W. Moncrieff, W. D. Collins, and J. T. Kiehl (1999), Long-term behavior of cloud systems in TOGA COARE and their interactions with radiative and surface processes. Part II: Effects of ice microphysics on cloud–radiation interaction, *J. Atmos. Sci.*, *56*(18), 3177–3195, doi:10.1175/1520-0469(1999)056<3177:LTBOCS>2.0.CO;2.

Xu, K.-M., and D. A. Randall (1995), Impact of interactive radiative transfer on the macroscopic behavior of cumulus ensembles. Part I: Radiation parameterization and sensitivity tests, *J. Atmos. Sci.*, *52*(7), 785–799, doi:10.1175/1520-0469(1995)052<0785:IOIRTO>2.0.CO;2.

Xu, K.-M., et al. (2002), An intercomparison of cloud-resolving models with the atmospheric radiation measurement summer 1997 intensive observation period data, *Q. J. R. Meteorol. Soc.*, *128*(580), 593–624, doi:10.1256/003590002321042117.

Zeng, X., W.-K. Tao, S. Lang, A. Y. Hou, M. Zhang, and J. Simpson (2008), On the sensitivity of atmospheric ensembles to cloud microphysics in long-term cloud-resolving model simulations, *J. Meteorol. Soc. Jpn.*, *86A*, 45–65, doi:10.2151/jmsj.86A.45.

Zhang, G. J., and N. A. McFarlane (1995), Sensitivity of climate simulations to the parameterization of cumulus convection in the Canadian climate centre general circulation model, *Atmos. Ocean*, *33*(3), 407–446, doi:10.1080/07055900.1995.9649539.